Journal of Template

Vol. 00, No. 0, 0000

Electrical Resistance Reduction of Laminated Carbon Fiber Reinforced Polymer by Dent made by indentation without cracking*

Akira TODOROKI*[1] Yasuhiro SHIMAZU*[2] and Yoshihiro MISUTANI*[3]

*[1] Department of Mechanical Sciences and Engineering
Tokyo Institute of Technology
2-12-1, Ookayama, Meguro-ku, Tokyo, Japan
E-mail: atodorok@ginza.mes.titech.ac.jp

*[2] Graduate student of Tokyo Institute of Technology
2-12-1, Ookayama, Meguro-ku, Tokyo, Japan

*3 Department of Mechanical Sciences and Engineering
Tokyo Institute of Technology
2-12-1, Ookayama, Meguro-ku, Tokyo, Japan

Abstract

Laminated carbon fiber reinforced polymer (CFRP) composites have been used in many aircraft components. Because it is quite difficult to detect delamination cracking visually, many cracking monitoring methods have been proposed. One of these methods is the self-sensing method, where electrical resistance change is used to detect the damage to the laminated CFRP. For a thick CFRP plate, however, a delamination crack is usually accompanied by a dent. The dent causes a decrease in the electrical resistance of the CFRP plate. Although dent monitoring using this decrease in electrical resistance has been proposed, it is also important to clarify the mechanism of the decrease in electrical resistance. In this study, therefore, experimental investigations were undertaken to understand the mechanism of the decrease in electrical resistance induced by the dent. An elastic-plastic finite element analysis was also performed to confirm the material deformation under the dent. We found that a decrease in the fiber spacing in the thickness direction caused by plastic deformation causes contact between the fibers, and this causes the decrease in the electric resistance in the thickness direction.

Key words: Dent, Electrical properties, Carbon fibers, Delamination

1. Introduction

Laminated carbon fiber reinforced polymer (CFRP) composites have been used in many aircraft components because of the high strength and stiffness per unit weight of these composites. Laminated CFRP composites, however, have a weak point in their interlaminar strength: delamination cracking is easily induced by slight impact loading. Because it is quite difficult to detect delamination cracking visually, many cracking monitoring methods have been proposed. One of these methods is a self-sensing method, where electrical resistance change is used to monitor the damage in the laminated CFRP composite. For the self-sensing method, the carbon fibers are used as sensors. Because the method does not require additional sensors, it is applicable to existing CFRP structures. The self-sensing method using electrical resistance change has been applied to detect damage in CFRP structures by many researchers [(1)-(20)].

*Received XX Xxx, 200X (No. XX-XXXX)
[DOI: 00.0000/ABCDE.2006.000000]

The authors used the self-sensing method to monitor delamination locations and dimensions: many electrodes were placed on the CFRP plate and the electrical resistance changes of multiple segments were measured to identify the delamination locations and dimensions [10, 11]. For a thin CFRP plate, delamination cracking impedes the electric current and causes increased electrical resistance [16]. For a thick CFRP plate, however, the delamination cracking is accompanied by a dent on the surface and the dent caused a decrease in the electrical resistance in the thickness direction of the CFRP plate [17]. The authors' group has revealed a dent monitoring process using the decreased electrical resistance caused by the dent [20]. The mechanism by which the dent reduces the electrical resistance in the thickness direction of the CFRP plate, however, has not been clarified. A dent causes a decrease in the electrical resistance, while delamination cracking causes increased electrical resistance: the effects are completely opposite to each other. However, without an understanding of this mechanism, it is quite difficult to monitor the dent location by using the measured electrical resistance change in any case.

In this study, therefore, two types of dent configuration, produced by indentation loading and pin loading processes, are investigated experimentally to clarify the mechanism by which the electrical resistance is decreased by a dent. The cross-sectional view of the dent is carefully observed and the fiber volume fractions under the dent are measured from the cross-sections under various loads. An elastic-plastic finite element method (FEM) analysis is also performed to confirm the material deformation under the dent. The decrease in electrical resistance is measured using a simple uniform model, and the decreases related to the two types of dent configuration are compared.

2. Experiments and Analysis

2.1 Experimental procedure

The material used here is the unidirectional carbon/epoxy PYROFIL MR380 prepreg made by Mitsubishi Rayon. Two types of stacking sequences were prepared here: quasi-isotropic laminates $[(0/90/\pm45)_2]$s and cross-ply laminates $[0_4/90_4]$s. The CFRP laminated plate is cured at 130°C and 0.6 MPa for 90 min in an autoclave. The thickness of the laminated CFRP plate is 3.2 mm. Two types of specimen were made for the present study: indentation-loading specimens and pin-loading specimens. The configuration of the indentation-loading specimen is shown in Fig. 1. The *x*-axis is the fiber angle of the 0° ply. The specimen length is 50 mm, and the width is 20 mm. Four electrodes are fabricated on the two surfaces, as shown in Fig. 1, to obtain an oblique electric current flow. A copper plating method is used here to make these electrodes [18].

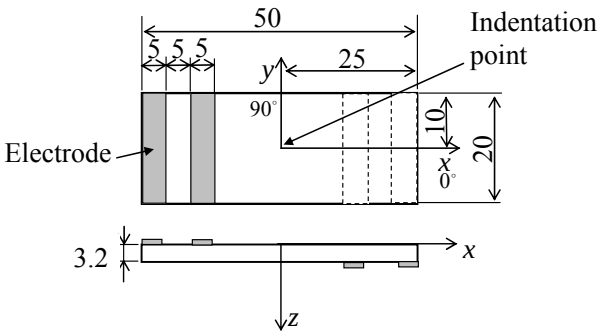

Fig.1 Indentation-loading specimen.

To investigate the effect of a dent alone, the dent must be made without producing matrix cracking or delamination cracking. To make a dent without cracking, a 1-mm-thick rubber sheet is placed under the specimen (a rubber sheet bed) on the metal jig plate and indentation loading tests are performed as shown in Fig. 2. Compression loading was applied at 0.5 mm/min up to loads of 1, 2, 3 and 4 kN. Five specimens were used for each test. An LCR meter (3533-50, Hioki Co.) was used to measure the electrical resistance changes. The electric current applied to measure the electrical resistance was 30 mA, and the frequency of the applied alternating electric current was 450 Hz. The two outer electrodes are used to apply the electric current, and the two inner electrodes are used to measure the voltage. The electric current flows along the oblique line in the thickness direction. At this low frequency, the phase angle was zero, and the CFRP is considered to be a simple resistance. The maximum dimensions and the depth of the dent were measured. After these measurements, the specimens were cut at the middle of each specimen (x=0), and the cross-sections were observed using a video microscope. From the cross-sectional view, inspection was carried out for damage such as matrix cracking and delamination cracking, and the local fiber volume fractions under the dent were measured using NI Vision Assistant version 8.5 image data processing software made by National Instruments.

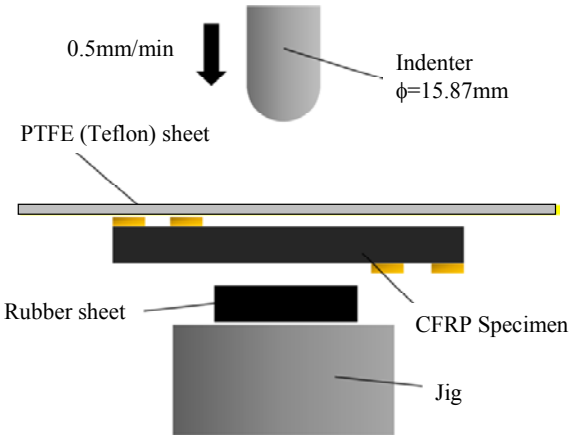

Fig.2 Indentation-loading test method.

The pin-loading type specimen is shown in Fig. 3. Similar to the procedure used for the indentation-loading specimens, to measure the local fiber volume fraction under the loading point, pin-loading was performed in alignment with the fiber direction on the x-axis (y=0). The specimen length was 50 mm and the width was 30 mm. To prevent pin-loading on the electrodes, each electrode was divided into two parts, as shown in Fig. 3. Electrodes #1 and #1' are coupled using a lead wire. Electrodes #2 and #2' are also coupled. Similar coupling arrangements are made for the other electrodes. The cross-ply laminates are used for the pin-loading specimen. The pin-loading configuration is shown schematically in Fig. 4.

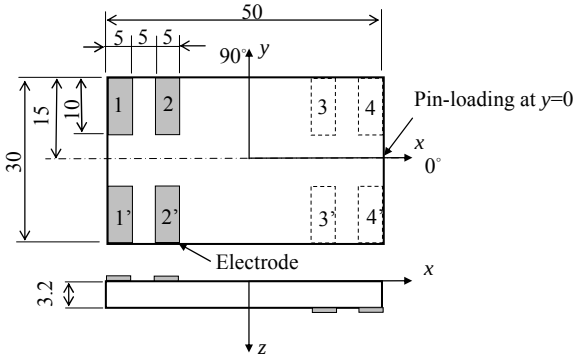

Fig.3 Pin-loading specimen configuration.

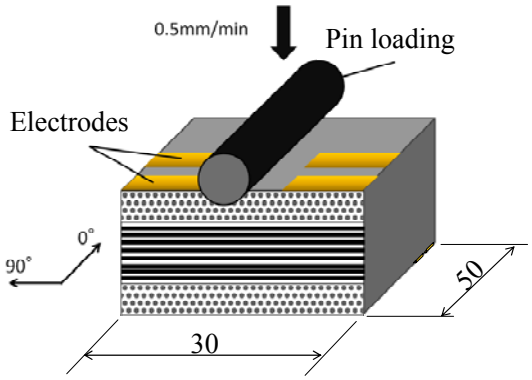

Fig. 4 Configuration of the pin-loading test.

Because it is possible to observe the cross-sectional view from the side surface for the pin-loading specimen, side surface cross-sectional observation was performed for this specimen. Because the loading area is wider than the indentation-loading specimen, the applied load was larger than the indentation loading, and three loading procedures were conducted up to 10, 20 and 30 kN. Over the 30kN, matrix cracking was observed. Similar measurements of the electrical resistance changes and the fiber volume fractions were performed for these specimens.

2.2 Elastic-plastic FEM analysis

To study the elastic-plastic deformation behavior of the specimen under pin-loading, a plane strain elastic-plastic FEM analysis was performed. Two-dimensional FEM analysis was performed using the commercially available FEM tool ANSYS ver.11.0. For the analysis, the six-node triangle elements of PLANE 183 were adopted. The mesh division is shown in Fig. 5. The diameter of the carbon fibers used is 6 μm, and the spacing between the fibers is set at 1.5 μm. Because small loading after the yielding of the epoxy resin is dealt with here, the analysis area is set as a small square of 112.5 μm, as shown in Fig. 5. Only half of the area is used for the analysis because of symmetrical deformation. The total number of nodes is approximately 20,000 and the total number of elements is approximately 8,700. At the bottom of the CFRP, the *z*-axis displacement is fixed to zero and the line is fixed at y=0, and the y direction displacement is fixed at zero. Contact elements are placed at the interface between the steel pin and the CFRP. The pin material is SS400 and the material properties of the epoxy resin and the carbon fiber are shown in Table 1. The steel pin and the carbon fibers are assumed to be perfectly elastic materials, and the epoxy resin is assumed to be an elastic-perfectly plastic material.

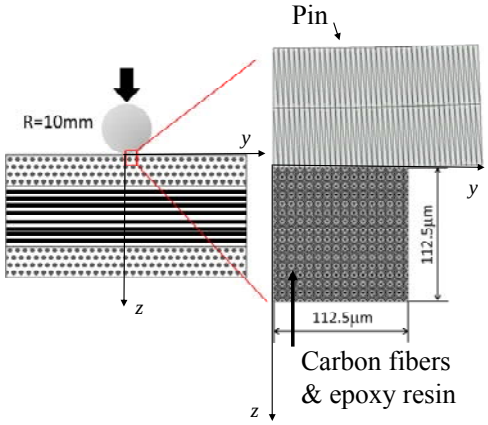

Fig.5 Mesh division of elastic-plastic FEM analysis.

Table 1 Material properties.

Material	Property	
SS400	E	206 GPa
	ν	0.3
	Yield stress	∞
Carbon fiber	E	380 GPa
	G	146 GPa
	ν_{xy}	0.3
	ν_{yz}	0.34
	Yield stress	∞
Epoxy resin	E	3 GPa
	ν	0.3
	Yield stress	100 MPa

2.3 Electric FEM analysis

To investigate the electric conductance change in the dent area, electric FEM analyses are performed here. For the 3D-FEM analyses, eight-node solid elements were adopted. At the electrodes, all surface nodes were coupled to have the same voltage, to simulate the copper electrodes. At the left electrode, an electric current of 1 A was applied, and the voltage of the right electrode was kept at zero. From the calculated voltage at the left electrode, electrical resistance was calculated. The element dimension was 1.25 mm (long)×1.25 mm (wide)×0.125 mm (thick). For the indentation loading specimen, the plate of 50mm×20mm×3.2mm is divided into 16,384 meshes. For the pin-loading specimen, the plate of 50mm×30mm×3.2mm is divided into 24,576 meshes. The material properties of the CFRP is σ_0=4100 S/m (fiber direction), σ_{90}=3.3 S/m (transverse direction), σ_t=3.3 S/m (thickness direction)[17]. The dent is modeled in the FEM analysis as a rectangular parallelepiped without the deformation of the dent but has higher electrical conductance. By increasing the σ_t of the dent region from the original value, the appropriate increased value of σ_t that matches experimental value is searched here.

3. Results and discussion

3.1 Indentation-loading specimens

Figures 6(a) and 6(b) show the typical dents after 4 kN indentation loading. For the isotropic laminate, the dent has an almost circular configuration, but the dent in the cross-ply laminate has an elliptical shape, although the difference is small. From outside observation, there is no additional damage to either specimen.

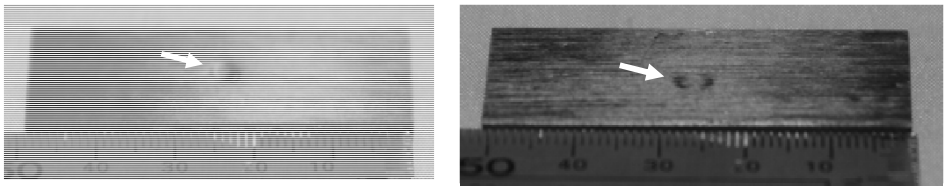

(a) Quasi-isotropic laminate. (b) Cross-ply laminate.

Fig. 6. Typical dent configuration after 4 kN loading.

Figure 7(a) shows the measured depth of the dent under various loads. The abscissa is the maximum load and the ordinate is the maximum depth measured after unloading. The standard deviation of the data is very small (approximately 10% of each data set). The circle symbols show the results for the quasi-isotropic laminates, and the triangle symbols show the results for the cross-ply laminates. The results show that there is no difference between the two results and the depth increases almost linearly with an increase in loading. Figure 7(b) shows the measured maximum dimension of the dent at the surface. The abscissa is the maximum load and the ordinate is the maximum dimension measured after unloading. Similar to the dent depth measurement results, it seems that there is no difference between the two results.

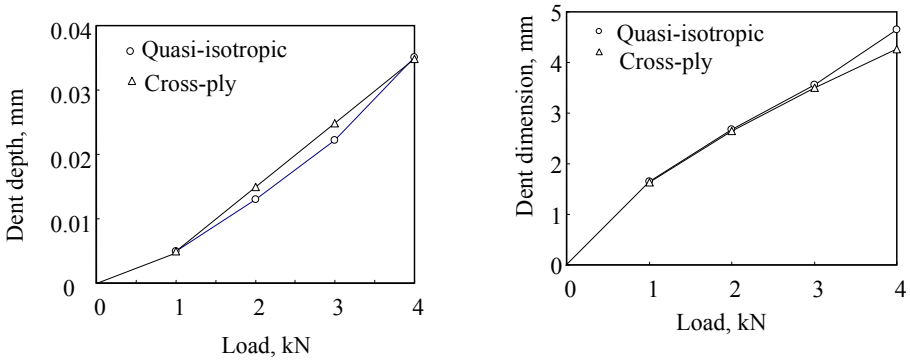

(a) Measured dent depth. (b) Measured maximum dimension of dent.

Fig. 7. Measured dent dimensions from the indentation tests.

Figure 8 shows the results for the electrical resistance change after unloading normalized by using the initial electrical resistance (electrical resistance change ratio). The abscissa is the load, and the ordinate is the measured electrical resistance change ratio. To investigate the electrical resistance change in the thickness direction caused by the dent, the electrical resistance values of the specimens are measured in the thickness direction using the oblique electric current path. The electrical resistance values in the thickness direction have a large scatter range. In this study, the standard deviation is shown by using the error bar for each point. As shown in Fig. 9, it is difficult to judge whether there is a difference between the results of the two stacking sequences because of the large scatter range. Based on a statistical test of 1%, the two results are judged to be similar. From these measured results, it can be said that the effect of the stacking sequence on the dent produced is negligible when compared with the data scatter. On the basis of these results, only the cross-ply laminates are used for the pin-loading specimens

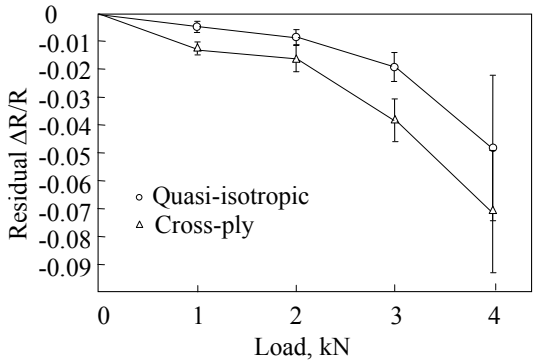

Fig.8 Electrical resistance change ratio of indentation-loading specimen.

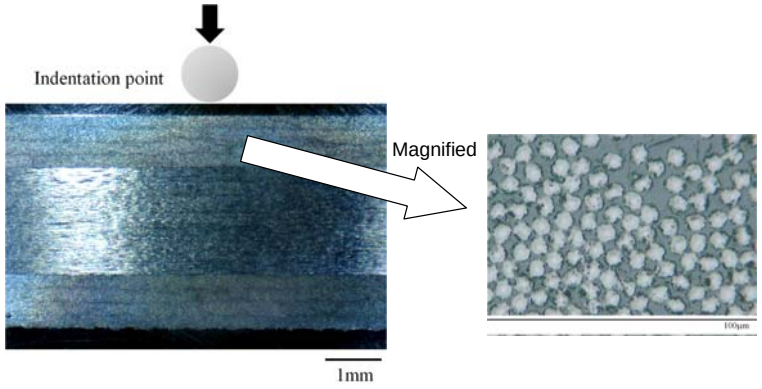

Fig.9 Cross-sectional views under the dent.

Figures 9 shows the cross-sectional view of the specimen under the dent. Figure 9 left shows that there is no matrix cracking or delamination cracking, because the indentation loading was performed using a rubber sheet bed to prevent cracking. Figure 9 right shows the magnified area just under the dent. This shows that there is no debonding between the fiber and the epoxy resin. These results show that the dent causes no damage in the CFRP because the rubber sheet bed was used to make the dent.

To investigate the fiber displacement caused by the dent, the local fiber volume fraction is measured from the cross-sectional view using image analysis. For these measurements, a small observation area gives better local variation but may also give a large scatter. First, therefore, the appropriate target image size was investigated with four types of image size using a specimen without a dent. The results show that the 150 μm square provides the smallest scatter, and is therefore adopted here.

Figure 10 shows the typical results for the local fiber volume fraction after loading. Figure 10(a) shows the results for 2 kN loading. Figure 10(b) shows the results for 4kN loading. The indentation loading was conducted at the point of origin of the x-axis. The results for the first ply have a large scatter because the first ply deforms greatly and has a resin-rich layer at the surface. The results for the first ply, therefore, are omitted in the later discussion. No change was observed in the small loading results. Figure 10(b) shows the higher volume fraction just under the dent, where the dent slightly increases the fiber volume fraction.

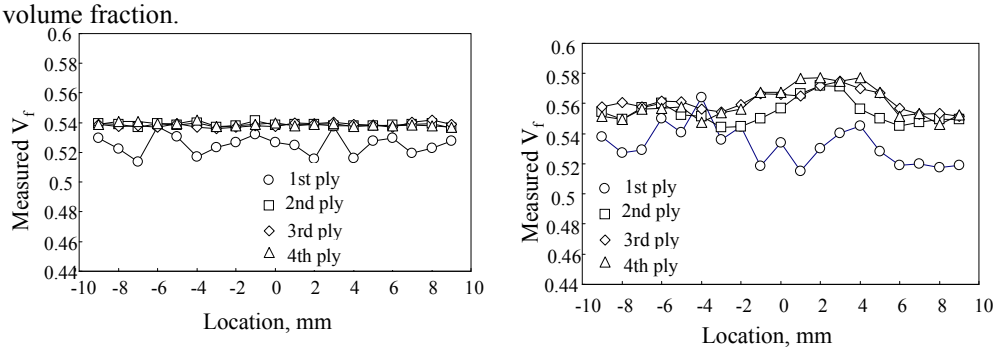

(a) Results of 2 kN loading. (b) Results of 4 kN loading.

Fig.10 Local fiber volume fraction after the loading of the indentation-loading specimen.

3.2 Pin-loading specimens

Figure 11 shows the results of the electrical resistance change ratio measurements. The abscissa is the applied load and the ordinate is the electrical resistance change ratio. Up to a load of 20 kN, the electrical resistance decreases linearly, but the electrical resistance change ratio decreases significantly at the 40 kN loading. Figure 12 shows the results for the dent depth. The abscissa is the applied load and the ordinate is the measured dent depth. The dent depth increases almost linearly with the increase in loading.

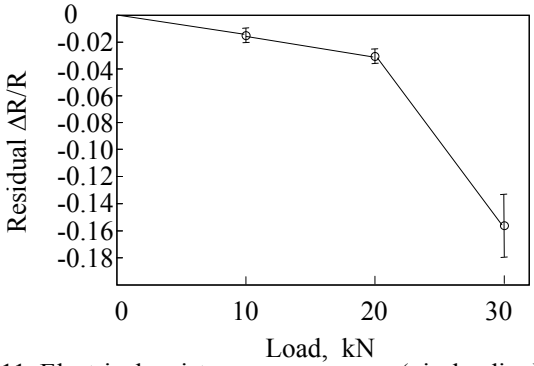

Fig. 11. Electrical resistance change ratio (pin-loading).

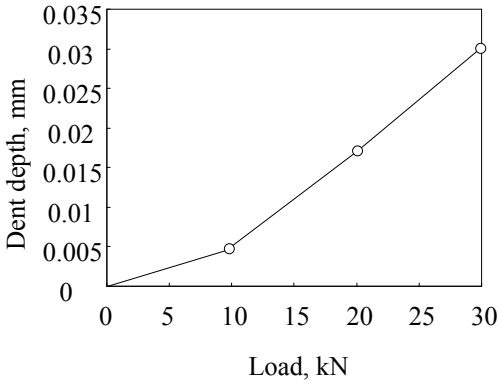

Fig. 12. Dent depth (pin-loading).

Because the first ply shows a large scatter, the local fiber volume fraction was measured after the second ply for the pin-loading specimen. Figure 13 shows the typical results for the measured local fiber volume fraction. The abscissa is the x-coordinate and the ordinate is the measured local fiber volume fraction. The pin loading was performed at the line where x=0. With increasing loading, the fiber volume fraction under pin loading increases more clearly than that under indentation loading. These results indicate that the dent causes an increase in the fiber volume fraction. The increase in the fiber volume fraction means a decrease in the fiber spacing.

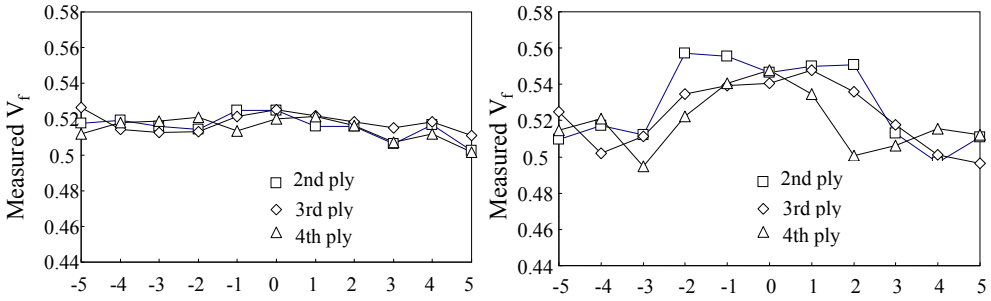

(a) Pin-loading of 10 kN. (b) Pin-loading of 30 kN.

Fig. 13. Local fiber volume fraction of pin-loading specimen.

3.3 Elastic-plastic FEM analysis

To investigate the fiber displacement caused by the dent, a plane-strain elastic-plastic FEM analysis was performed. The applied load was a pin displacement of 1.5 μm in the z-direction. The results are shown in a contour plot in Fig. 14. As the material property is not the measured one, this deformation FEM analysis is just a qualitative one.

The red color indicates high equivalent stress. As shown in Fig. 14, a stress concentration occurs at the fibers because of their higher elastic modulus in comparison with the epoxy resin, and the epoxy resin under the fiber yields. This means that only the fiber spacing in the z-direction shrinks because of the resin yielding. The small increase in the fiber volume fraction observed in the experiments seems to be as a result of the shrinkage of the fiber spacing in the z-direction. The decrease in the fiber spacing in the z-direction causes an increase in fiber contact in the thickness direction, and this causes an increase in the electric conductance in the z-direction. Because the fiber displacement in the y-direction is negligible compared with the displacement in the z-direction, the electric conductance change is limited to the thickness direction. To obtain the exact analysis, we need exact properties and three-dimensional FEM analysis. This is our future work.

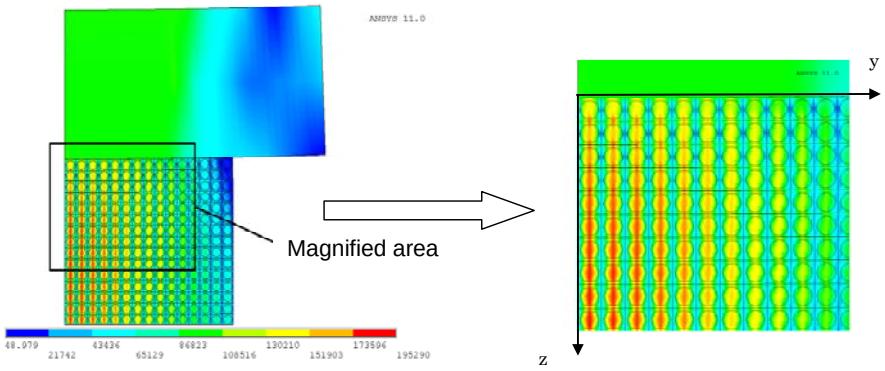

Fig. 14. Equivalent stress distribution obtained using the plane-strain elastic-plastic FEM analysis.

3.4 Electric conductance analysis of electric conductance

To estimate the change in electric conductance, several electrical FEM analyses were performed. As shown in the previous sections, the dent causes the fiber spacing to decrease under the dent area, and this causes an increase in the electric conductance (decrease of electric resistance). To simplify the estimation process, let us consider the affected region to be limited to a rectangular solid of uniform electric conductance in the thickness direction. Three-dimensional steady state electric current FEM analyses were performed by changing the electric conductance in the thickness direction of the dent-affected rectangular solid. Equivalent electric conductances of σ_t that give the similar electrical-resistance changes of the experimental results are obtained here. Because the experimental results show that the fiber spacing only shrinks in the thickness direction, only the electric conductance in the thickness direction is changed until the electric resistance change ratio becomes the measured result. The equivalent electric conductance values obtained are shown in Fig. 15. The results for both the indentation-loading specimen and the pin-loading specimen are shown in Fig. 15. The abscissa is the dent depth and the ordinate is the estimated electric conductance when using the rectangular solid model.

Because the thickness of a single ply is 0.2 mm, small dents up to 10% of the ply thickness cause a linear increase in the electric conductance with increasing dent depth. In this small dent region, the loading type, such as indentation loading or pin loading, does not affect the increase in the electric conductance. For larger dents, however, the electric conductance is no longer located on the linear line. This may be caused by differences in plastic deformation behavior between the different loading types. Further research is essential to clarify the relationships between the dents caused by various imparter projectiles and the electric conductance changes for deeper dents.

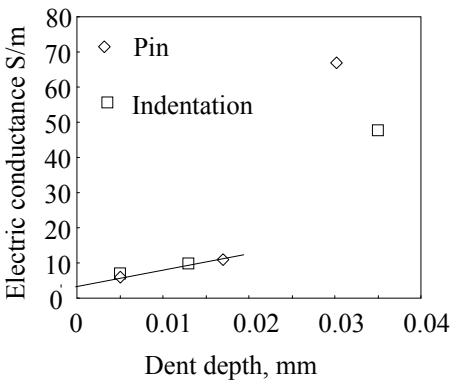

Fig. 15. Estimation results for electric conductance in the thickness direction under the dent area.

4. Conclusions

For thick CFRP laminates, delamination cracking is usually accompanied by a dent. The dent causes a decrease in the electrical resistance. Although dent monitoring using this decrease in electrical resistance had been proposed, the mechanism had not been clarified. The present study focuses on the mechanism of the decrease in electric resistance caused by a dent after impact loading. Indentation-loading specimens and pin-loading specimens were experimentally investigated by measuring the electrical resistance changes. The fiber volume fraction of the local area was measured under the dent using the cross-sectional view. The results obtained are as follows.

(1) The effect of the stacking sequence on the dent depth, dimensions and electric resistance change is small when compared with the scatter of the experimental results.

(2) The dent causes a reduction in the spacing between the fibers in the thickness direction, and this causes an increase in fiber contact. The increased fiber contact causes a decrease in the electrical resistance in the thickness direction.

(3) When the dent is small compared with the ply thickness, the loading conditions do not affect the decrease in electrical resistance. The decrease in electrical resistance for a large dent, however, is affected by the loading type.

References

(1) K. Schulte, and Ch Baron, Load and Failure Analyses of CFRP Laminates by Means of Electrical Resistivity Measurements, *Composites Science and Technology*, Vol.36, No.1, (1989), pp.63-76.

(2) N. Muto,, H. Yanagida, T. Nakatsuji,, M. Sugita,, and Y. Ohtsuka,, Preventing Fatal Fractures in Carbon-Fibre – Glass-Fibre-Reinforced Plastic Composites by Monitoring Change in Electrical Resistance, *J. American Ceramic Society,* Vol.76, No.4, (1993), pp.875-879.

(3) A.S. Kaddoour, F.A., Al-Salehi, and S.T.S. Al-Hassani, Electrical Resistance Measurement Technique for Detecting Failure in CFRP Materials at High Strain Rate, *Composites Science and Technology*,Vol.51, No.3, (1994),pp. 377-385.

(4) X. Wang and D.D.L. Chung, Short Carbon Fiber Reinforced Epoxy as a Piezoresistive Strain Sensor, *Smart Materials and Structures*, Vol.4, No.4, (1995), pp.363-367 .

(5) A. Todoroki, K. Matsuura, and H. Kobayashi, Application of Electric Potential Method to Smart Composite Structures for Detecting Delamination, *JSME International J., Series A,* Vol.38, No.4, (1995), pp.524-530.

(6) P.E. Irving, C. Thiagarajan, Fatigue Damage Characterization in Carbon Fibre Composite Materials using an Electrical Potential Technique. *Smart Materials and Structures,* Vol.7, No.4, (1998), pp.456-466.

(7) D.C. Seo, and J.J. Lee, Damage Detection of CFRP Laminates using Electrical Resistance Measurement and a Neural Network, *Composite Structures,* Vol. 47, No.1-4, (1999), pp.525-530.

(8) J.C. Abry, Y.K. Choi, A. Chateauminois, B. Dalloz , G. Giraud, M. Salvia, In-situ Monitoring of Damage in CFRP Laminates by using AC and DC measurements, *Composite Sciences and Technology*, Vol.61, No.6, (2001), pp.855-864.

(9) J.B. Park, T. Okabe, N. Takeda, W.A. Curtin, Electromechanical modeling of unidirectional CFRP composites under tensile loading condition, *Composites Part A,* 2002, Vol.33, No.2, (2002), pp.267-275.

(10) A. Todoroki, Y. Tanaka, and Y. Shimamura, Delamination monitoring of graphite/epoxy laminated composite plate of electric resistance change method, *Composites Science and Technology,* Vol.62, No.9, (2002), pp.1151-1160.

(11) A. Todoroki, M. Tanaka, Y. Shimamura, Measurement of orthotropic electric conductance of CFRP laminates and analysis of the effect on delamination monitoring with electric

resistance change method, *Composite Sciences and Technology*, Vol.62, No.5, (2002), pp.619-628.

(12) K. Ogi, Y. Takao, Characterization of piezoresistance behavior in a CFRP unidirectional laminate, *Composites Science and Technology*, Vol.65, No.2, (2005), pp.231-239.

(13) N. Angelidis, and P.E. Irving, Detection of impact damage in CFRP laminates by means of electrical potential techniques, *Composites Science and Technology*, 2007;Vol.67, No.3–4, (2007), pp.594–604.

(14) E.Sevkat, B. Liaw, and F.A. Delale, Statistical model of electrical resistance of carbon fiber reinforced composites under tensile loading, *Composites Science and Technology*, Vol.68, No.10–11, (2008),pp.2214–2219.

(15) I. De Baere, W. Van Paepegem, and J. Degrieck, Electrical resistance measurement for in situ monitoring of fatigue of carbon fabric composites, *International Journal of Fatigue*, Vol.32, No.1, (2010), pp.197–207.

(16) A. Todoroki, Y. Samejima, Y. Hirano, R. Matsuzaki, and Y. Mizutani, Mechanism of electrical resistance change of a thin CFRP beam after delamination cracking, *Journal of Solid Mechanics and Materials Engineering, JSME*, 2010, Vol.4, No.1, (2010), pp.1-11.

(17) A. Todoroki, A., Y. Samejima, Y. Hirano, R. Matsuzaki and Y. Mizutani, Electrical Resistance Change of Thick CFRP Laminate for Self-Sensing, *Journal of Solid Mechanics and Materials Engineering JSME,* Vol.4, No. 6, (2010), pp.658-668.

(18) A.Todoroki,, K.Suzuki, Y. Mizutani, and R. Matsuzaki, Durability Estimates of Copper Plated Electrodes for Self-sensing CFRP Composites, *Journal of Solid Mechanics and Materials Engineering JSME*, 2010, Vol.4, No.6, (2010), pp.610-620.

(19) A. Todoroki, K. Suzuki, Y. Mizutani and R. Matsuzaki, Electrical Resistance Change of CFRP under compression load, *Journal of Solid Mechanics and Materials Engineering JSME*, Vol. 4, No.7, (2010), pp.864-874.

(20) A. Todoroki, Y. Shimazu, Y. Mizutani, and R. Matsuzaki,, Using electrical resistance change to monitor the damage in a thick CFRP plate caused by a dent, *Journal of Solid Mechanics and Materials Engineering, JSME*, Vol.5, No.1, (2011), pp.44-53.